Submitted to J. Am. Ceram. Soc.

UCRL-18762 Rev.
Preprint

cy. 2

# MECHANICAL PROPERTIES AND FRACTURE BEHAVIOR OF CHEMICALLY BONDED COMPOSITES

Mark A. Stett and R. M. Fulrath

RECEIVED
LAWRENCE
RADIATION LABORATORY

JUL 23 1969

LIBRARY AND
DOCUMENTS SECTION

May 1969

TWO-WEEK LOAN COPY

*This is a Library Circulating Copy which may be borrowed for two weeks. For a personal retention copy, call Tech. Info. Division, Ext. 5545*

LAWRENCE RADIATION LABORATORY
UNIVERSITY of CALIFORNIA BERKELEY

cy. 2

UCRL-18762 Rev.

## DISCLAIMER

This document was prepared as an account of work sponsored by the United States Government. While this document is believed to contain correct information, neither the United States Government nor any agency thereof, nor the Regents of the University of California, nor any of their employees, makes any warranty, express or implied, or assumes any legal responsibility for the accuracy, completeness, or usefulness of any information, apparatus, product, or process disclosed, or represents that its use would not infringe privately owned rights. Reference herein to any specific commercial product, process, or service by its trade name, trademark, manufacturer, or otherwise, does not necessarily constitute or imply its endorsement, recommendation, or favoring by the United States Government or any agency thereof, or the Regents of the University of California. The views and opinions of authors expressed herein do not necessarily state or reflect those of the United States Government or any agency thereof or the Regents of the University of California.

# MECHANICAL PROPERTIES AND FRACTURE BEHAVIOR OF CHEMICALLY BONDED COMPOSITES

Mark A. Stett and R. M. Fulrath

Inorganic Materials Research Division, Lawrence Radiation Laboratory, and Department of Materials Science and Engineering, College of Engineering, University of California, Berkeley, California

## ABSTRACT

May 1969

The effect of chemical bonding between phases of a glass matrix-metal composite on the strength and fracture behavior was investigated. When no chemical bonding occurs, strengthening can be achieved through the mechanical formation of an interface between the dispersant and matrix. By the formation of a chemical bond, an even greater strengthening can be obtained. Strengthening occurs by the limitation of the Griffith flaw size and is controlled by micromechanical stress concentrations developed upon loading. Internal stresses developed upon cooling from the fabrication temperature control the path of fracture. The existence of a chemical bond serves to counteract the micromechanical stress concentration and therefore increase the strength.

# I. INTRODUCTION

Many of today's new materials are multiphase or composite in nature. Dispersion strengthened alloys make use of a finely divided second phase distributed in a crystalline matrix. Glass-ceramics make use of controlled crystallization from a glassy melt. Glass fiber reinforced resins are used extensively in organic matrix composites. The properties of composite materials will depend upon the properties of the individual components, their distribution, and their physical and chemical interaction.

In understanding the properties of brittle-matrix composites, the obvious choice for the matrix is glass--the ideal brittle material. Fulrath[1] demonstrated that by vacuum hot-pressing powdered glass, a continuous matrix of glass containing a dispersed phase could be fabricated. Since that time extensive studies on the elastic and mechanical properties of such systems were reported.[2-13] In all the previous studies the interfacial bonding characteristics between the dispersion and the matrix were not clearly identified.

Nason[3] first encountered the problem of interfacial bonding in attempting to disperse tungsten and nickel microspheres in glass matrices where the matrix thermal expansion coefficient was selected to be either less than or greater than that of the dispersion. When the thermal expansion coefficient of the glass was less than that of the nickel metal and there was no bonding between phases, the nickel shrank away from the glass upon cooling and formed pseudoporosity. Composites fabricated by Nason from tungsten and a glass of lower thermal expansion coefficient, however, showed an anomalous strengthening. He then hot-pressed this

glass under the same conditions against a well-polished disk of tungsten. Adherence was observed between the tungsten and glass. A similar experiment using a nickel disk and another glass with a lower thermal expansion coefficient than that of nickel showed no adherence.

Bertolotti and Fulrath[10] used this thermal expansion mismatch and lack of interfacial bonding in order to create a controlled amount of spherical porosity of known size in their investigation of the strength of porous glass. With small particle sizes, they also observed an anomalous strengthening and proposed that adsorbed water on the surface of the glass powder used in fabricating the composite caused a slight oxidation of the nickel surface and resulted in a bond between the oxidized nickel and the glass. As a result of this observation, a more extensive study of the effect of a chemical bond between phases in a brittle matrix composite was undertaken.

## II. THEORY

In attempting to analyze a brittle matrix system, we must consider two types of stresses. Internal stresses are created between glassy and crystalline phases during cooling from fabrication temperature as a result of the difference in the thermal expansions of the two phases. Under mechanical loading, differences in the elastic properties of individual components can lead to a localized concentration of the applied stress. The existence of a bond between phases further complicates the situation.

It has often been proposed that internal stresses affect the mechanical strength of composite materials. Fulrath[1] showed that internal stresses could be detected in ceramic bodies by X-ray diffraction techniques. After correction for beam penetration and camera geometry, peak shifts

give an accurate measurement of strain. An increase in diffraction angle is indicative of compression while a decrease in angle corresponds to tension. A more detailed analysis of the technique and examples of its application were presented by Grossman and Fulrath.[14]

Theoretical solutions exist for stress concentrations associated with elastic inhomogeneities of various shapes in an infinite matrix under load. Since glass fracture is usually nucleated at the specimen surface and because of the high stress gradients away from the surface in the strength test, Goodier's solutions[15] for a circular inclusion in a flat plate were used in this study.

For a circular hole in a plate it is found that the expression for the tangential stress concentration yields tensile stresses greater than the applied stress under conditions of tensile load. The expression for this stress concentration is

$$\sigma_t = 2T\left[\frac{R^2}{4r^2} - \frac{3R^4}{4r^4}\cos 2\theta\right] + T\sin\theta \qquad (1)$$

where T = applied tensile load

$\theta$ = angle from direction of applied tension = 90° for maximum stress concentration in this case

R = hole radius

r = radius under consideration

For a simple tension, T, in one direction there is a maximum stress concentration of 3T as can be seen in Fig. 1. This stress concentration decreases rapidly to only 1.2T at a distance of R into the matrix. The stress concentration also decreases rapidly with $\theta$ from the 90° maximum,

confining the stress concentration to small regions at A and B.

In the case of a rigid inclusion, contact with the surrounding material produces a different type of stress concentration. A rigid inclusion in simple tension induces a tension at C and D which can be as much as 1.5T. The expression for this stress concentration is:

$$\sigma_r = 2G_G \left[ -\frac{A}{r^2} + \left( \frac{3B}{r^4} - \frac{2C}{r^2} \right) \cos 2\theta \right] + \frac{T}{2} (1 + \cos 2\theta) \qquad (2)$$

where

$$A = \frac{TR^2}{4G_G} \; \frac{(1-2\mu_M)G_G - (1-2\mu_G)\, G_M}{(1-2\mu)G_G + G_M} \qquad (3)$$

$$B = \frac{TR^4}{4G_G} \; \frac{G_G - G_M}{G_G + (3-4\mu_G)G_M} \qquad (4)$$

$$C = \frac{TR^2}{2G_G} \; \frac{G_G - G_M}{G_G + (3-4\mu_G)(G_M} \qquad (5)$$

In these expressions

$\theta$ = 0° for maximum stress concentration

$G_G$ = bulk modulus of the glass

$G_M$ = bulk modulus of the metal dispersed phase

and the other terms as previously defined. The tension at A and B is reduced and becomes compression if $\mu_G$ is less than 0.25. The tensile stress concentration at C and D also decreases with increasing r. A stress concentration of 1.08T is reached at a distance of 4R. The stress

concentration once again decreases with a change in $\theta$ from $\theta = 0°$, confining the stress concentration to regions at C and D.

A bond is obtained between a glass and a metal when the glass is saturated with the oxide of the metal at the glass-metal interface. According to Pask and Fulrath[16] a chemical bond can occur when a balance of bond energies is achieved across the transition zone at the interface between the glass and the metal. This balance occurs when "thermodynamic equilibrium" is obtained at the interface. By "thermodynamic equilibrium," it is meant that each of the phases is saturated with the lower oxide and that there is no possibility of further reaction to form a new phase. If the available oxide is entirely dissolved by the glass before the glass attains the saturation concentration, the resultant contact with a purely metallic surface results in a weak bond.

Hasselman and Fulrath[7] have hypothesized that a dispersion of a hard second phase within a brittle glass matrix will strenghen the composite by limiting the size of Griffith flaws. When the average distance between second phase particles is less than the flaw size, the flaw size is limited to this average mean free path. For a flat plate containing an elliptical flaw, the Griffith expression for the macroscopic strength, $S_o$, is

$$S_o = \left( \frac{4\gamma E}{\pi a} \right)^{1/2} \qquad (6)$$

where $\gamma$ is the surface energy, E is Young's modulus of elasticity, and "a" is the flaw size. An expression for the mean free path, d, between spherical particles of uniform radius, R, distributed statistically

throughout a matrix was provided by Fullman[17] as

$$d = \frac{4R\,(1-\phi)}{3\phi} \tag{7}$$

where $\phi$ is the volume fraction of dispersed particles. Substituting Eq. (7) into Eq. (6) we find the strength of a composite that is being strengthened by a flaw limitation mechanism to be

$$S_o = \left(\frac{3\gamma E\phi}{\pi R(1-\phi)}\right)^{1/2} \tag{8}$$

When a given load is applied to the composite there will be, due to the stress concentrations resulting from differences in elastic properties of the phases,[9] areas of higher stress than the applied load. The measured strength will therefore be

$$S_m = \frac{1}{K}\,S_o \tag{9}$$

By substituting Eq. (9) into Eq. (8) and rearranging this to isolate the variable, $(1/d)^{1/2}$, we find

$$S_m = \left(\frac{4\gamma E}{\pi K}\right)^{1/2} \left(\frac{3\phi}{4R(1-\phi)}\right)^{1/2} \tag{10}$$

This function was plotted by first calculating the slope from approximate values of K (1.4), $\gamma$ (10,000 ergs/cm$^2$), and E ($10^7$ psi). The assumption of 10,000 ergs/cm$^2$ for the fracture surface energy falls within the very wide range of values previously assumed or measured in other investigations.

This value of the surface energy is, however, an assumption and more confidence could be expressed as to its accuracy only if a more detailed study of the fracture surface energy were available. From Eq. (10) it can be seen that this function will necessarily go through the origin. The location of the horizontal portion of the curve (where the dispersion does not limit the flaw size) can be found by determining the strength of an abraded glass. The horizontal extension of the individual glass strength value will intersect the plotted slope at the size of the Griffith flaw. This behavior can be seen in Fig. 2. In order to assure strengthening in the composites studied here, a combination of particle size and volume fraction was chosen in each case that provided an average mean free path less than the Griffith flaw size developed by a standard abrasion treatment of all tensile surfaces.

## III. EXPERIMENTAL PROCEDURE

The glasses used in this investigation were made in the laboratory from silica flour, reagent grade sodium carbonate and boric acid, and alumina. The materials were dry mixed and then melted and refined in a platinum crucible at 1400°C in an electric furnace. Densities of the cast glass were measured using an Archimedes technique with methyl alcohol. The cast glass was crushed and dry ground to -325 mesh in an alumina-lined ball mill with alumina pebbles. Elastic properties of the glasses were measured by the resonance technique of Spinner and Tefft[18] and Pickett.[19] With this method, two values for Young's modulus were obtained for each specimen by calculations using Hasselman's[20] tables. The shear moduli were calculated from an expression of the pertinent shape factor given by Spinner and Tefft.[18] A summary of material properties is given in Table 1.

Nickel microspheres were purchased and partitioned by screening into various size fractions in order to obtain desired average particle sizes. In order to evaluate the various oxidation treatments, weight gain tests were carried out at three temperatures. The curves that were obtained were predominantly linear in the ranges that were used and can be seen in Fig. 3. Scanning electron micrographs of both oxidized and unoxidized spheres are shown in Fig. 4.

The composites were prepared from thoroughly mixed combinations of oxidized nickel spheres and powdered glass and were vacuum hot pressed at 500 or 1000 psi for either 10 or 20 minutes at 700°C. The hot-pressing arrangement was described previously. The similar softening characteristics of the three glasses permitted the fabrication of theoretically dense composites at a single temperature.

Samples for the measurement of elastic properties were cut with a diamond saw from a 2 in. diameter x 1/4 in. thick vacuum hot-pressed glass disk. Strength measurements were made on .160 in. x .050 in. bars of various lengths that were cut from a 2 in. x .050 in. vacuum hot-pressed disk. The thin disks were cooled in an argon atmosphere to avoid cracking. An adequate flaw density was insured by abrading the tensile surface of the disk lightly with 240 grit SiC. Thermal expansion bars were also cut from the 2 in. diameter x 1/4 in. thick vacuum hot-pressed glass disks.

Uniaxial strengths were measured using a four-point loading device with a 3/4 in. overall span. Specimens were loaded with the abraded surface as the tensile surface. Several breakings were made with each specimen to obtain an average strength value. Resultant fracture surfaces

were examined using a scanning electron microscope. Preparation included coating of the specimens with a 100-200Å layer of aluminum.

Hot-pressed samples were sectioned and mounted in a clear casting resin. All samples were polished with a set of silicon carbide papers (240, 400, and 600 grit) and then finished on a series of diamond pastes (6, 2 and 1/2 micron diamond). Carbon was vapor deposited on the finished samples to provide a conductive surface suitable for electron microprobe analysis. The microprobe was used to examine the migration of the nickel oxide into the matrix glass.

## IV. RESULTS AND DISCUSSION

### (1) D Glass System ($\alpha_G < \alpha_{Ni}$)

The system that was initially selected to investigate the effect of bonding on the strength of glass-metal composites was that used by Bertolotti and Fulrath.[10] Nickel microspheres that were pre-oxidized to varying degrees were used in conjunction with D glass in order to expand upon the anomalous strengthening observed for small particle sizes. It can be seen in Fig. 2 that a particle radius of 25μ and a volume fraction of 20% are sufficient to position the oxidized nickel-D glass system to the right of point A. The strength of the composite should, therefore, be a function of the mean free path in the matrix as calculated using Eq. (8). Either the residual or micromechanical stress concentrations may modify this calculated strength and would be reflected in the value of K in Eq. (9). Composites with a series of pre-oxidation treatments ranging from 0.18 to 5.8% weight gain were fabricated at 500 psi for 10 minutes at 700°C. Strengths of these samples are given in Table 2 and can be seen as a function of the amount of pre-oxidation in Fig. 5.

(A) Non-bonded Composites: When there was a lack of bonding between the D glass and the nickel, the nickel shrank away from the D glass upon cooling from the fabrication temperature. This led to the formation of pseudoporosity and the resultant weakening of the composite. Since the two phases were not in contact, no internal stresses were introduced. The previously mentioned X-ray strain measurement technique was used to qualitatively determine the state of internal stress in this non-bonded D glass-nickel composite which provided a standard for comparison with other systems. Location of the nickel (420) peak was taken as a gauge of the internal stress. It can be seen in Table 3 that the nickel (420) peak was located at 144.52°2θ.

The hypothesis was presented that the effect of micromechanical stress concentrations on the strength of a brittle material depends on the size of the Griffith flaw relative to the region over which the stress concentration acts.[9] The Griffith flaw size generated by the standard specimen preparation technique used here can be obtained from point A in Fig. 2 and was found to be 150μ. By comparing this value with the 50μ diameter pseudoporosity formed in this case we would expect only a slight decrease in strength upon the addition of the first pore. The data confirm this expectation with a glass strength of 7,790 psi and a measured composite strength of 6,440 psi.

Fracture surfaces of the broken bars were examined using a scanning electron microscope and can be seen in Fig. 6. The path of fracture in a brittle material is altered by the inclusion of particles of a second phase or pores. If the inclusion is a pore, the fracture will propagate to the pore and around its diameter, leaving a hemispherical cavity in

the fracture surface. It can be seen in Fig. 6a that the fracture propagated directly to and around the sphere because of the tensile stress concentrations around a spherical cavity.

(B) Bonded Composites. When a bond was created between the D glass and the nickel, the shrinkage of the nickel away from the glass upon cooling was prevented. The thermal contraction did, however, introduce a radial tensile stress which was evidenced in the X-ray strain measurements of Table 3 where the nickel (420) peak was shifted to 144.39° 2θ. This radial tensile internal stress was formed hydrostatically around the nickel sphere. It can be seen also from the strength data in Fig. 5 that the bond does, indeed, prevent the shrinkage of the nickel away from the glass and provide strengthening in a normally porous system.

The maximum stress concentration due to loading developed in this system was calculated using the following values and Eqs. (2-5):

$G_G$ = 337 kbar (measured for D glass)

$G_M$ = 724 kbar (measured for nickel)

$\mu_G$ = 0.2 (calculated for D glass)

$\mu_M$ = 0.4 (calculated for nickel)

$R = 25\mu = 9.84 \times 10^{-4}$ in.

Maximum stress concentration will occur at the interface and will be 1.348T for this system. Verification of the net radial tensile stress is seen in the scanning electron micrographs of the fracture surfaces (Fig. 6) showing fracture through the matrix and around the spheres rather than radially to the spheres. Had contact been maintained between the glass and the metal without the presence of a bond, this value of stress concentration would have been used in the strength calculation

using Eq. (9).

The shape of the curve in Fig. 5 for the ten minute series corresponds to the bond hypothesis presented previously. An optimum bond (and also optimum strength) was observed. A pre-oxidation treatment of about 0.8% weight gain followed by the given hot-pressing treatment saturated the glass with nickel oxide at the sphere-glass interface. With lesser pre-oxidation treatments, the glass was less than saturated and a lower strength value was observed.

With greater pre-oxidation treatments, a bulk oxide layer remained after saturation and the strength was correspondingly less. For a given pre-oxidation treatment, the greater length of time at temperature will allow more oxide to diffuse away from the particle, thus shifting the peak to greater weight gain. An increased pre-oxidation will be needed to yield the optimum amount of remaining oxide layer. In order to test this hypothesis in the oxidized nickel-D glass system, a series of samples with varied pre-oxidation treatments was hot pressed at 700°C and 500 psi for 20 minutes. The data are presented in Table 4 and the effect is clearly seen in Fig. 5. The optimum pre-oxidation was increased, but the reason for the decrease in the maximum strength is not clear.

A sample with 1.1% weight gain was examined using an electron beam microprobe in order to determine the extent of diffusion of the oxide into the glass. Nickel counts were taken from the center of a sphere radially outward into the glass matrix. It was found from three randomly selected spheres that nickel was present to a distance of approximately 15μ from the sphere.

A calculation of the expected strength was made using Eq. (9). When contact was maintained between the glass and the nickel, the applied tensile load tended to pull the glass away from the nickel and micromechanical stress concentrations arose. The presence of a bond, however, tended to counter this separation and a simple strengthening due to a limitation of the flaw size was observed (K=1). Using the following values for the D glass-nickel system,

$\theta = 0.2$

$R = 25\mu = 9.84 \times 10^{-4}$ in.

$E = 11.7 \times 10^{6}$ psi (measured)

$\gamma = 10{,}000$ ergs/cm$^2$ = 0.0566 lb/in. (assumed)

$K = 1$

Eq. (9) gave an expected measured strength of 12,680 psi. This agrees well (5.2% error) with the maximum measured value of 12,020 psi in Table 3. It therefore appears that the strength of the composite system was not determined by internal stresses but rather by the micromechanical stress concentrations developed in loading.

Representative fracture surfaces of bonded composites can be seen in Fig. 6. The path of fracture was altered when a chemical bond exists between the glass and the nickel. The fracture propagated through the glass around the inclusion, but still within the glass. This propagation through the matrix was most evident in the case of the optimum bond (Fig. 6d). Because of the thermal expansion variation among the saturated glass at the interface, the nickel, and the matrix glass, a radial internal tensile stress was developed in the matrix. To relieve this tension, a fracture propagated around the sphere at a finite distance in

the glass phase.

(2) S Glass System ($\alpha_G = \alpha_{Ni}$)

An attempt was made to compound a glass whose thermal expansion coefficient was equal to that of nickel. The measured value of thermal expansion for S glass was $13.8 \times 10^{-6}$ in./in. °C which is very nearly the $13.9 \times 10^{-6}$ in./in. °C of nickel. In the following discussion they are considered close enough to be equal, but it should be recognized that the glass expansion was very slightly less than that of the nickel. In the S glass-nickel system it was necessary to change the particle size and volume fraction in order to remain in the flaw-limitation region. A particle size of 30μ and a volume fraction of 30 vol. % were selected in order to remain to the right of point B in Fig. 2. Once again a series of composites was hot-pressed at 1000 psi for 10 minutes at 700°C with a wide range of pre-oxidation treatments. The data are given in Table 5 and can be seen in Fig. 7.

(A) Non-bonded Composites. With matching expansions it would be expected that no internal stresses would be created upon cooling the composite from the fabrication temperature. X-ray strain measurements in Table 3 show the nickel (420) peak to be found at 144.51° 2θ. By comparison with the non-bonded D glass standard of 144.52° 2θ there are essentially no internal stresses created in fabrication.

Since contact was mechanically maintained between the glass and the metal upon cooling, stress concentrations were only created on loading. A calculation of these stress concentrations was made using the following values and Eqs. (2-5):

$G_G$ = 277 kbars (measured for S glass)

$G_M$ = 724 kbars (measured for nickel)

$\mu_G$ = 0.2 (calculated for S glass)

$\mu_M$ = 0.4 (calculated for nickel)

$R = 30\mu = 11.8 \times 10^{-4}$ in.

For an applied load of T, the maximum stress concentration as shown in Fig. 1 was 1.374T. Once again the maximum stress concentration was expected to occur at the interface. This concentration of stress meant that, for an applied load of T, there was an area (shown in Fig. 1) within the composite where a stress of 1.374T was developed.

The expected strength was calculated using Eq. (9) and recalling that stress concentrations existed as a result of the maintenance of contact between sphere and glass upon cooling from the fabrication temperature. Using the stress concentration factor of 1.374T and a measured Young's modulus of $9.8 \times 10^6$ psi, a value of 10,110 psi was calculated for the non-bonded composite. This compares well (2.7% error) with the average measured value of 10,380 psi that was found for the nine bars that were broken.

Scanning electron micrographs of the fracture surfaces of the broken bars can be seen in Fig. 8. In the absence of a bond it can be seen (Fig. 8a) that the fracture propagated to the sphere and around it at the sphere-glass interface. Hemispherical cavities remain as evidence of spheres in the opposite fracture surface.

(B ) Bonded Composites. In the D glass system the bond played an important role in that it prevented the shrinkage of the nickel away from the glass. With matching thermal expansions, however, this role was

unnecessary and the bond had no effect upon internal stresses. This is evidenced by the X-ray strain measurements of Table 3 which showed no shift of the nickel (420) peak with the formation of a bond. The same location, 144.51° 2θ, was observed as for the non-bonded case.

The shape of the curve for the 30 vol. % series in Fig. 7 once again shows an optimum pre-oxidation treatment in order to obtain the optimum bond and therefore the maximum strength for the given fabrication process. With lesser pre-oxidation treatments we once again saw a lower strength because saturation was not reached. With greater pre-oxidation treatments, a bulk oxide layer remained after saturation and a lower strength was observed. In order to illustrate the necessity of controlling the average mean free path between particles, a series to the left of point B in Fig. 2 with only 20 vol. % of 25μ diameter spheres was hot-pressed. In this instance the flaw-limitation mechanism was not applicable and we expected to see little effective strengthening upon the addition of the second phase. The results of this series are given in Table 6 and can be seen in Fig. 7.

The expected strength of a bonded S glass-nickel composite was calculated using Eq. (9). Once again it was observed that the presence of a bond counteracted the concentration of stress developed during loading. Using

$\phi = 0.3$

$R = 30\mu = 11.8 \times 10^{-4}$ in.

$E = 9.8 \times 10^{6}$ psi

$K = 1$

the strength to be expected was calculated as 13,900 psi. The maximum

measured value in Table 5 is 12,460 psi and this is 10.3% lower than anticipated.

It is evident, as in the D glass system, that the proper amount of pre-oxidation in order to obtain the maximum strength is critical. Just slightly more or less than the optimum pre-oxidation will yield a much weaker composite.

Characteristic fracture surfaces of the 30 vol. % bonded composites are seen in Fig. 8. Once again a small radial tension was developed as a result of the slight thermal expansion variation among the saturated glass, the nickel, and the matrix glass. The bond is evident in Fig. 8b-d by observing glass adhering to the nickel spheres in the fracture surface. Its magnitude can be compared with the bonded D glass-nickel system shown in Fig. 6.

A sample with 0.9% weight gain was examined with the electron beam microprobe. Nickel counts were taken as the beam traversed radially from the center of a sphere outward into the matrix. Three randomly selected spheres yielded a distance of 13μ from the sphere at which nickel was detected.

(3) M Glass System ($\alpha_G > \alpha_{Ni}$)

The third system to be investigated was one in which the thermal expansion of the glass is greater than that of the nickel. In this case the interface between the glass and the second phase was formed mechanically by the contraction of the glass around the sphere during cooling. In addition, a chemical bond was introduced by the pre-oxidation process. Once again a change in the volume fraction of 35 vol. % of 30μ spheres was dictated in order to preserve the flaw-limitation mechanism (Fig. 2)

and remain to the right of point C. A series of composites was hot-pressed at 1000 psi for 10 minutes at 700°C with a range of pre-oxidation treatments. The strength values are given in Table 7 and can be seen in Fig. 9.

(A) Non-bonded Composites. With the thermal expansion coefficient of the glass greater than that of the nickel, the glass contracted around the nickel microspheres upon cooling from the fabrication temperature. This contraction around the nickel was sufficient to put the nickel into a slight compression as is evidenced by the X-ray strain measurements in Table 3. The nickel (420) peak was detected at 144.54° 2θ compared with 144.52° 2θ for the non-bonded D glass standard.

Only mechanical contact was maintained between the glass and the nickel in the non-bonded composite. Under the applied tension the tendency of the glass to pull away from the nickel gave rise to a micromechanical stress concentration. The maximum stress concentration in this system was calculated using the following values and Eqs. (2-5).

$G_G$ = 290 kbars (measured for M glass)

$\mu_G$ = 0.2 (calculated for M glass)

$R = 30\mu = 11.8 \times 10^{-4}$ in.

$\phi = 0.35$

When a load of T was applied to the composite, a stress concentration of 1.366T was formed at the glass-nickel interface as shown in Fig. 1.

Equation (9) was used to calculate the strength to be expected from the non-bonded composite. Using the calculated stress concentration factor and a measured value of $10.2 \times 10^6$ psi for the Young's modulus, a strength of 11,610 psi was predicted. This agrees very well (2.1% error)

with the actual measured value of 11,860 psi for the twelve bars broken.

Fracture surfaces of the broken bars in the M glass-nickel system were examined with the scanning electron microscope. The fracture path in the non-bonded case can be seen in Fig. 10a. Once again the fracture propagated toward the nickel and around it, leaving a hemispherical cavity in the fracture surface. This was expected because it relieved the biaxial tension resulting from the internal stress.

(B) Bonded Composites. As in the case of the matching thermal expansion system, the existence of a bond did not affect the internal stresses. This was illustrated by the X-ray strain measurements which located the nickel (420) peak at 144.55° 2θ for the bonded composite compared with 144.54° 2θ for the non-bonded composite.

The presence of a bond greatly enhanced the strength of composites in this system. As can be seen in Fig. 9, strengthening was limited until a pre-oxidation treatment was used which would saturate the glass under the hot-pressing conditions. A sample made with spheres pre-oxidized to 0.9% weight gain was examined with the electron microprobe. Nickel was detected to a distance of 18μ from the glass-nickel interface.

Existence of the bond again prevented the glass from pulling away from the nickel under an applied tensile load (K=1). Equation (9) yielded a predicted strength of 15,880 psi for the bonded composite. A comparison of this value with the maximum strength measured in Table 7 of 15,390 psi again shows a good (3.1% error) agreement for the 14 samples broken.

Representative fracture surfaces of the bonded composites in the M glass-nickel system can be seen in Fig. 10. The radial compression

introduced as an internal stress during fabrication correspondingly set up a tangential tensile stress. In order to attempt to relieve this tangential tensile stress, the fracture proceeded directly to the nickel microspheres and around them at the glass-nickel interface in spite of the presence of the bond. Careful examination of the pictures shows (as in Fig. 10e) some adhesion of the glass to the microspheres confirming the existence of a bond.

## V. SUMMARY

Composites were hot-pressed using glasses of varying thermal expansion coefficient and nickel with varying degrees of pre-oxidation in order to study the effect of chemical bonding between the nickel and glass upon strength and fracture behavior. Glasses with a thermal expansion coefficient lower than, higher than, and matching that of nickel were compounded. The bond was developed by the migration of oxide at the fabrication temperature and the resultant saturation of the glass with the oxide in the vicinity of the nickel.

When no bond was present, a low expansion glass led to pseudo-porosity with the resultant weakening, and a high expansion glass led to strengthening due to mechanical contraction of the glass around the nickel upon cooling. No matter what the relative thermal expansions were, micromechanical stress concentrations were developed upon loading. Strengthening was observed with both matching and high thermal expansion glasses, but the micromechanical stress concentrations reduced the strength far below that expected from a simple Griffith flaw limitation mechanism.

The presence of the optimum bond between phases dramatically

increased the strength of the composites. In the case of the low expansion glass the bond prevented the formation of pseudoporosity by halting shrinkage of the nickel away from the glass. In all cases the existence of a bond between phases counteracted the micromechanical stress concentrations developed upon loading. The strength was then dictated by a simple Griffith flaw limitation mechanism.

Internal stresses that were developed within the composite during cooling from the fabrication temperature controlled the path of fracture. Differences in thermal expansion created either radial or tangential tension in the matrix. In order to relieve tangential tension, such as that developed in the bonded, high expansion matrix system, the fracture propagated directly to the nickel sphere. In order to relieve radial tension, such as that developed in the bonded, low expansion matrix system, the fracture propagated around the nickel, but still within the glass matrix.

The strength and path of fracture were found to be independent. Internal stresses controlled the path of fracture, micromechanical stress concentrations controlled the strength, and the bond counteracted the micromechanical stress concentrations to produce an even greater strength.

## ACKNOWLEDGMENT

The scanning electron microscope used was operated within the Electronics Research Laboratory, University of California. It was purchased under Grant No. GB-6428 from the National Science Foundation and is operated under Grant No. GM15536 from the National Institute of Health.

Thanks are extended to Mike Nemanic for assistance with the scanning electron microscope and to George Dahl for help in specimen preparation.

This work was done under the auspices of the U. S. Atomic Energy Commission.

REFERENCES

1. R. M. Fulrath, "Internal Stresses in Model Ceramic Systems," J. Am. Ceram. Soc., 42 (9) 423-429 (1959).

2. L. A. Jacobson, "Strength of a Two-Phase Model System" (M.S. Thesis) University of California, Berkeley, 1959.

3. D. O. Nason, "Effect of Interfacial Bonding on Strength of a Model Two-Phase System" (M.S. Thesis), University of California, Berkeley, 1962.

4. P. L. Studt and R. M. Fulrath, "Mechanical Properties and Chemical Reactivity in Mullite-Glass Systems," J. Am. Ceram. Soc., 45(4) 182-188 (1962).

5. D. P. H. Hasselman and R. M. Fulrath, "Effect of Alumina Dispersions on Young's Modulus of a Glass," J. Am. Ceram. Soc., 48(4) 218-219 (1965).

6. D. P. H. Hasselman and R. M. Fulrath, "Effect of Spherical Tungsten Dispersions of Young's Modulus on a Glass," J. Am. Ceram. Soc., 48 (10) 548-549 (1965).

7. D. P. H. Hasselman and R. M. Fulrath, "Proposed Fracture Theory of a Dispersion-Strengthened Glass Matrix," J. Am. Ceram. Soc., 49 (2) 68-72 (1966).

8. G. Einmahl, "Strength in a Two-Phase Model System with Fiber Reinforcement" (M.S. Thesis), University of California, Berkeley, 1966.

9. D. P. H. Hasselman and R. M. Fulrath, "Micromechanical Stress Concentrations in Two-Phase Brittle Matrix Ceramic Composites," J. Am. Ceram. Soc., 50 (8) 399-404 (1967).

10. R. L. Bertolotti and R. M. Fulrath, "Effect of Micromechanical Stress Concentrations on Strength of Porous Glass," J. Am. Ceram. Soc. 50 (11) 558-562 (1967).

11. M. A. Stett and R. M. Fulrath, "Chemical Reaction in a Hot-Pressed $Al_2O_3$ Glass Composite," J. Am. Ceram. Soc. 50 (12) 673-676 (1967).

12. M. A. Stett and R. M. Fulrath, "Strengthening by Chemical Bonding in a Brittle Matrix Composite," J. Am. Ceram. Soc., 51 (10) 599-600 (1968).

13. Y. Nivas, "Limitation of Griffith Flaws in Glass-Matrix Composites" (M.S. Thesis), University of California, Berkeley, 1968.

14. L. N. Grossman and R. M. Fulrath, "X-ray Strain Measurement Techniques for Ceramic Bodies," J. Am. Ceram. Soc., 44 (11) 567-71 (1961).

15. J. N. Goodier, "Concentration of Stress Around Spherical and Cylindrical Inclusions and Flaws," J. Appl. Mech., 1 (1) 39-44 (1933).

16. J. A. Pask and R. M. Fulrath, "Fundamentals of Glass-to-Metal Bonding: VIII," J. Am. Ceram. Soc., 45 (12) 592-96 (1962).

17. R. L. Fullman, "Measurement of Particle Sizes in Opaque Bodies," Trans. AIME, 197 (3) 447-52 (1953).

18. S. Spinner and W. E. Tefft, "Method for Determining Mechanical Resonance Frequencies and for Calculating Elastic Moduli from these Frequencies," Am. Soc. Testing Mater. Proc., 61, 1221-38 (1961); Ceram. Abstr. 1962, October, p. 248g.

19. G. Pickett, "Equations for Computing Elastic Constants from Flexural and Torsional Resonant Frequencies of Vibrations of Prisms and Cylinders," Am. Soc. Testing Mater. Proc., 45, 846 (1945).

20. D. P. H. Hasselman, "Tables for Computation of Shear Modulus and Young's Modulus of Elasticity from Resonant Frequencies of Rectangular Prisms," The Carborundum Company, Niagara Falls, New York, 1962.

Table I

Material Properties

| Material | Composition | Thermal Expansion in/in °Cx10$^6$ $\alpha$ | Young's Modulus psi x 10$^{-6}$ E | Poisson's Ratio $\mu$ | Density gm/cc $\rho$ |
|---|---|---|---|---|---|
| Ni | | 13.9 | 30.0 | 0.42 | 8.9 |
| D glass | 70 $SiO_2$<br>14 $B_2O_3$<br>16 $Na_2O$ | 7.7 | 11.7 | 0.2 | 2.47 |
| S glass | 55 $SiO_2$<br>15 $Al_2O_3$<br>30 $Na_2O$ | 13.8 | 9.8 | 0.2 | 2.47 |
| M glass | 50 $SiO_2$<br>13 $Al_2O_3$<br>37 $Na_2O$ | 16.0 | 10.2 | 0.2 | 2.51 |

Table II

Crossbending strength and statistical data for oxidized nickel-D glass composites (10 min.)

| Oxidation Temp(°C) | Oxidation Time (hrs.) | Weight Gain (%) | Average Strength (psi) | Number of Samples | Standard Deviation (% of average) |
|---|---|---|---|---|---|
| 800 | 1/4 | 0.3 | 10,730 | 17 | 8.4 |
| " | 1/2 | 0.7 | 11,960 | 17 | 6.2 |
| " | 1 | 1.1 | 12,020 | 18 | 9.5 |
| " | 2 | 1.7 | 10,870 | 15 | 12.6 |
| " | 3 | 2.2 | 10,910 | 9 | 11.7 |
| " | 4 | 2.8 | 10,030 | 17 | 13.4 |
| " | 6 | 3.3 | 10,350 | 19 | 10.6 |
| " | 12 1/4 | 5.8 | 10,260 | 12 | 12.2 |
| 750 | 1/6 | 0.18 | 9,560 | 18 | 13.7 |
| " | 1/2 | 0.3 | 10,190 | 19 | 12.1 |
| " | 1 1/2 | 0.9 | 11,740 | 21 | 7.0 |
| " | 2 | 1.1 | 11,440 | 22 | 7.3 |
| " | 15 | 3.6 | 10,390 | 18 | 5.4 |
| D glass alone | | | 7,740 | 36 | 13.5 |
| D glass & unoxidized Ni | | | 6,440 | 32 | 8.1 |

TABLE III

Internal stress measurements

| | $2\theta$ | d |
|---|---|---|
| D glass ($\alpha_G < \alpha_{Ni}$) | | |
| No bond | 144.52 | 0.80870 |
| Bond | 144.39 | 0.80900 |
| S glass ($\alpha_G = \alpha_{Ni}$) | | |
| No bond | 144.51 | 0.80873 |
| Bond | 144.51 | 0.80873 |
| M glass ($\alpha_G > \alpha_{Ni}$) | | |
| No bond | 144.54 | 0.80866 |
| Bond | 144.55 | 0.80863 |

TABLE IV

Crossbending strength and statistical data for oxidized nickel-D glass composites (20 min.)

| Oxidation Temp(°C) | Oxidation Time (hrs.) | Weight Gain (%) | Average Strength (psi) | Number of Samples | Standard Deviation (% of average) |
|---|---|---|---|---|---|
| 750 | 1/2 | 0.3 | 8,030 | 18 | 7.3 |
| " | 1 | 0.6 | 7,780 | 13 | 15.9 |
| " | 1 1/2 | 0.9 | 9,390 | 14 | 15.2 |
| " | 3 | 1.4 | 10,750 | 18 | 10.7 |
| " | 4 | 1.7 | 9,830 | 18 | 10.6 |
| " | 15 | 3.6 | 9,670 | 16 | 9.9 |
| D glass alone | | | 7,740 | 36 | 13.5 |
| D glass & unoxidized Ni | | | 6,440 | 32 | 8.1 |

TABLE V

Crossbending strength and statistical data for oxidized nickel-S glass composites (30% spheres)

| Oxidation Temp(°C) | Oxidation Time (hrs.) | Weight Gain (%) | Average Strength (psi) | Number of Samples | Standard Deviation (% of average) |
|---|---|---|---|---|---|
| 750 | 1/6 | 0.18 | 10,690 | 14 | 5.6 |
| 750 | 1/2 | 0.3 | 11,410 | 15 | 5.2 |
| 750 | 1 | 0.6 | 12,460 | 11 | 6.4 |
| 800 | 1/2 | 0.7 | 10,790 | 16 | 9.0 |
| 750 | 1 1/2 | 0.9 | 11,540 | 13 | 3.5 |
| 750 | 2 | 1.1 | 11,090 | 13 | 5.3 |
| 750 | 4 | 1.7 | 11,000 | 17 | 9.2 |
| 800 | 3 | 2.2 | 10,690 | 11 | 8.1 |
| 750 | 10 | 2.8 | 10,570 | 17 | 8.6 |
| 800 | 6 | 3.3 | 9,870 | 13 | 6.8 |
| 750 | 15 | 3.6 | 9,850 | 13 | 8.1 |
| S glass only | | | 8,140 | 24 | 9.2 |
| S glass & unoxidized Ni | | | 10,380 | 9 | 8.2 |

TABLE VI

Crossbending strength and statistical data for oxidized nickel-S glass composites (20% spheres)

| Oxidation Temp (°C) | Oxidation Time (hrs.) | Weight Gain (%) | Average Strength (psi) | Number of Samples | Standard Deviation (% of average) |
|---|---|---|---|---|---|
| 750 | 1/6 | 0.18 | 9,280 | 13 | 4.7 |
| 750 | 1/2 | 0.3 | 9,230 | 17 | 9.8 |
| 750 | 1 | 0.6 | 9,040 | 12 | 13.6 |
| 750 | 1 1/2 | 0.9 | 8,940 | 11 | 4.8 |
| 750 | 2 | 1.1 | 9,320 | 20 | 9.0 |
| 750 | 3 | 1.4 | 8,860 | 15 | 6.8 |
| 750 | 4 | 1.7 | 8,690 | 16 | 9.6 |
| 800 | 3 | 2.2 | 8,740 | 16 | 14.1 |
| 750 | 10 | 2.8 | 9,460 | 19 | 10.9 |
| 750 | 15 | 3.6 | 9,410 | 19 | 7.9 |
| S glass only | | | 8,140 | 24 | 9.2 |
| S glass & unoxidized Ni | | | 8,770 | 18 | 6.0 |

TABLE VII

Crossbending strength and statistical data for oxidized nickel-M glass composites (10 min.)

| Oxidation Temp (°C) | Oxidation Time (hrs.) | Weight Gain (%) | Average Strength (psi) | Number of Samples | Standard Deviation (% of average) |
|---|---|---|---|---|---|
| 750 | 1/6 | 0.18 | 13,630 | 20 | 9.4 |
| 750 | 1/2 | 0.3 | 14,240 | 16 | 6.1 |
| 750 | 1 | 0.6 | 15,260 | 19 | 6.1 |
| 800 | 1/2 | 0.7 | 14,580 | 7 | 8.8 |
| 750 | 1 1/2 | 0.9 | 15,000 | 17 | 10.9 |
| 750 | 2 | 1.1 | 14,800 | 11 | 5.3 |
| 750 | 4 | 1.7 | 15,390 | 14 | 5.2 |
| 800 | 3 | 2.2 | 15,120 | 9 | 7.3 |
| 750 | 15 | 3.6 | 15,320 | 10 | 6.9 |
| M glass only | | | 9,920 | 13 | 6.1 |
| M glass & unoxidized Ni | | | 11,860 | 12 | 7.0 |

## FIGURE CAPTIONS

Figure 1. Stress concentrations developed under an applied tensile load (----- = porosity, _____ = inclusion).

Figure 2. Calculated composite strength as a function of reciprocal square root of the average mean free path.

Figure 3. Oxidation of nickel spheres.

Figure 4. Nickel spheres before and after oxidation (20°, 1380X)
(A) Unoxidized; (B) Oxidized 1 hr. at 750°C (0.6%)

Figure 5. Strength as a function of weight gain for the D glass-oxidized nickel series.

Figure 6. Fracture surfaces in the D glass (10 min) series (inclined 20°, marks indicate 25μm)
(A) 0%, (B) 0.18%, (C) 0.3%, (D) 0.7%, (E) 1.7%, (F) 5.8%.

Figure 7. Strength as a function of weight gain for the M glass-oxidized nickel series.

Figure 8. Fracture surfaces in the S glass (70% glass) series (inclined 20°, marks indicate 50μm)
(A) 0%, (B) 0.18%, (C) 0.9%, (D) 1.7%, (E) 2.2%, (F) 3.3%.

Figure 9. Strength as a function of weight gain for the M glass-oxidized nickel series.

Figure 10. Fracture surfaces in the M glass series (inclined 20°, marks indicate 50μm)
(A) 0%, (B) 0.18%, (C) 0.3%, (D) 0.9%, (E) 1.7%, (F) 2.2%.

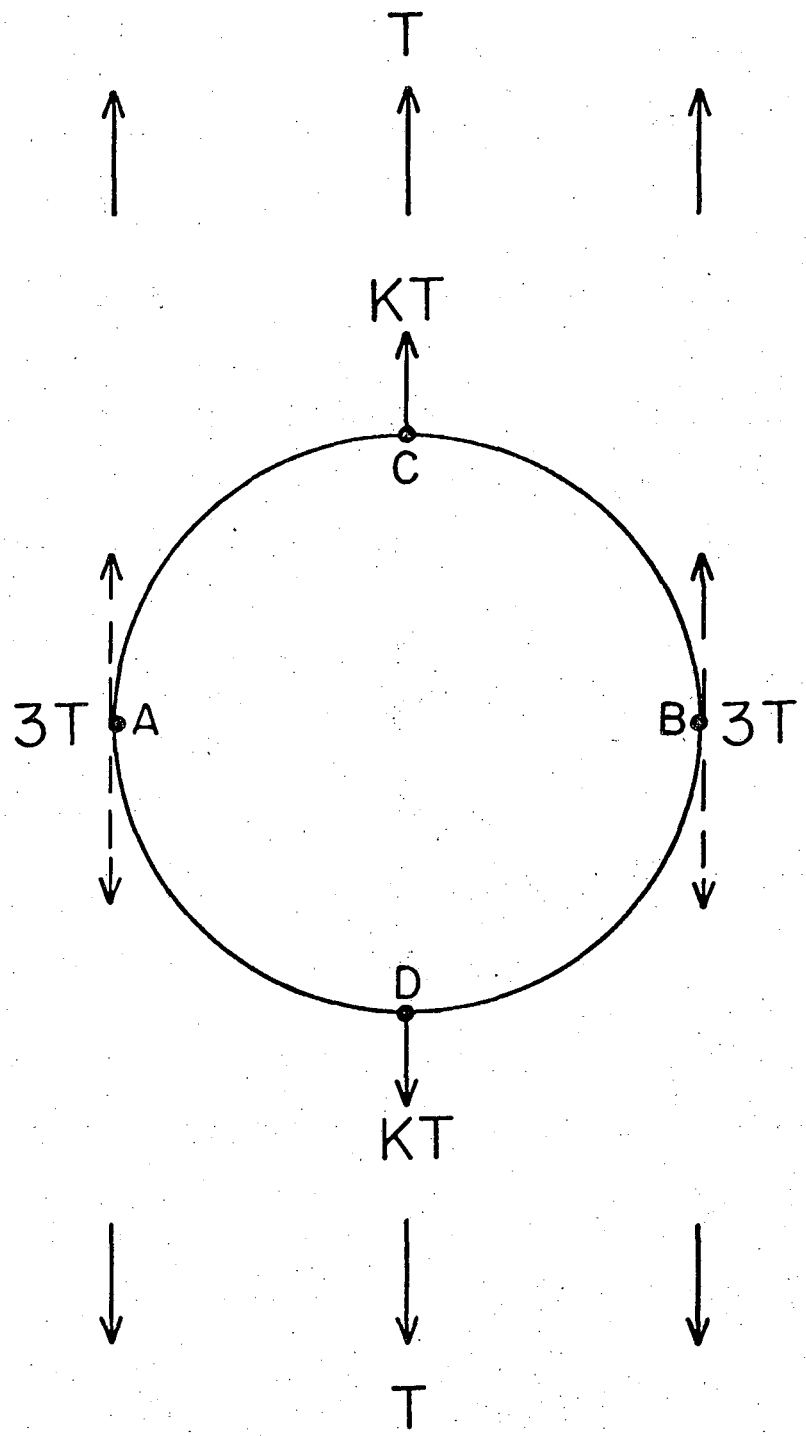


XBL 695-451

Fig. 1

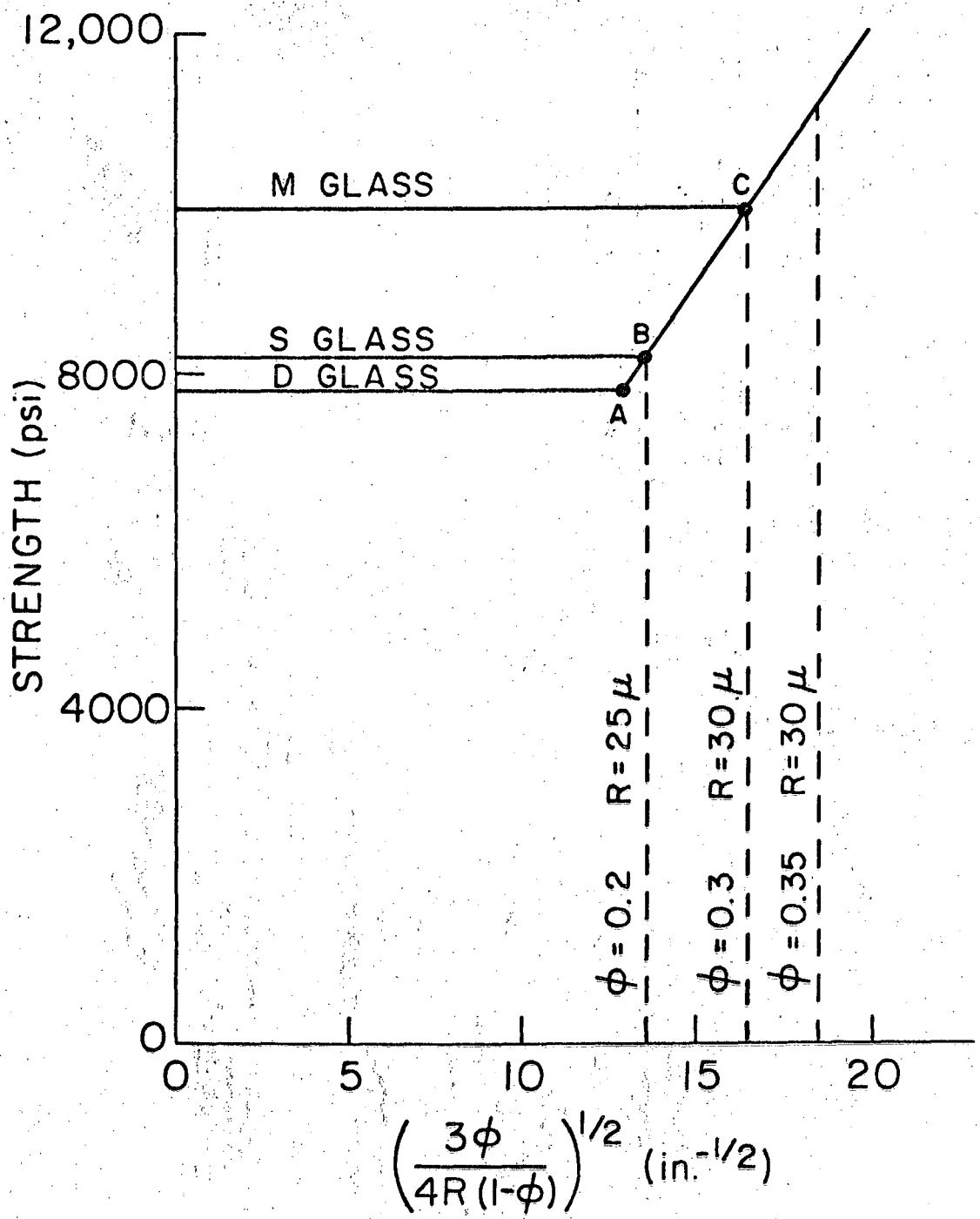


XBL 695-458

Fig. 2

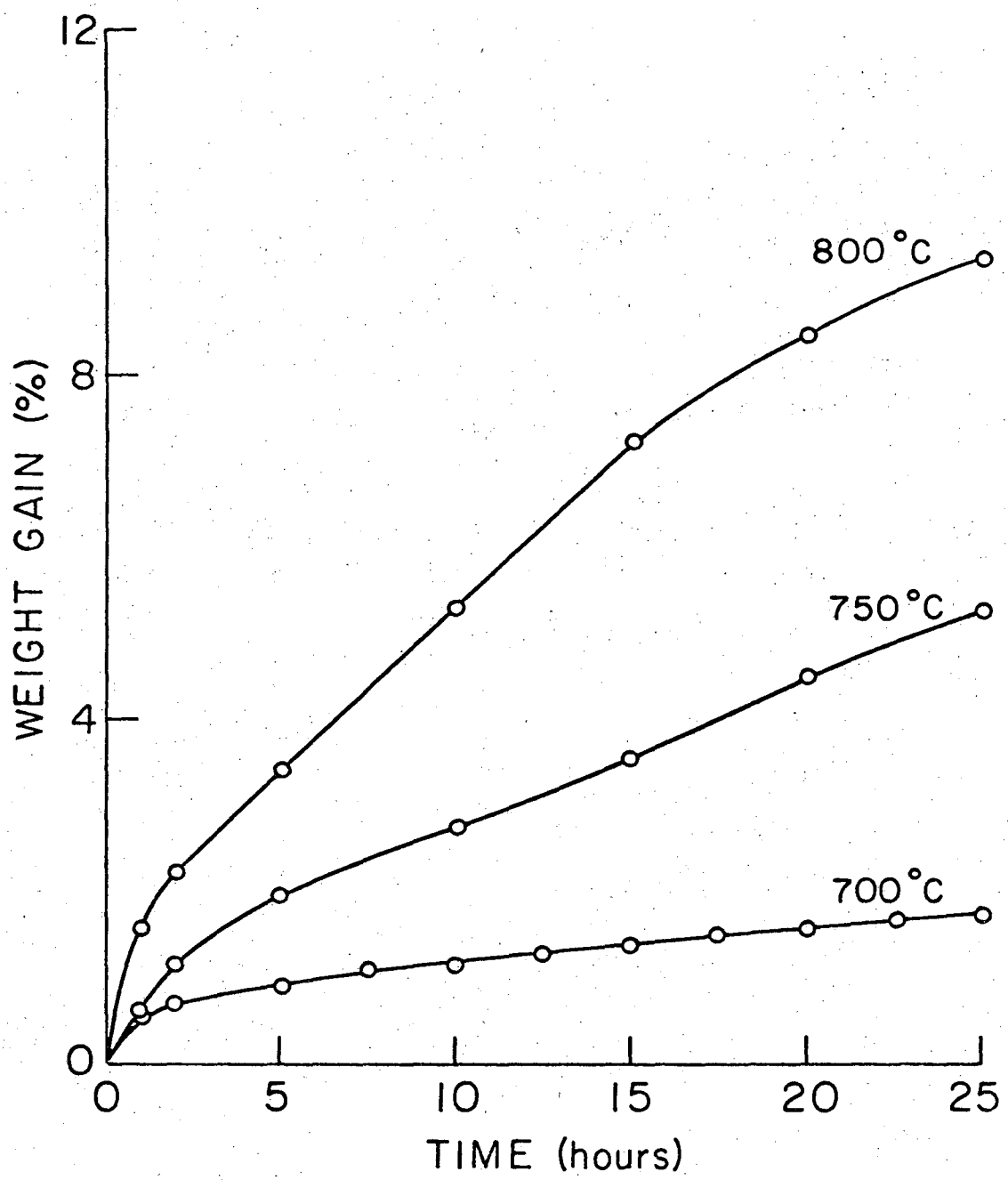


XBL 695-455

Fig. 3

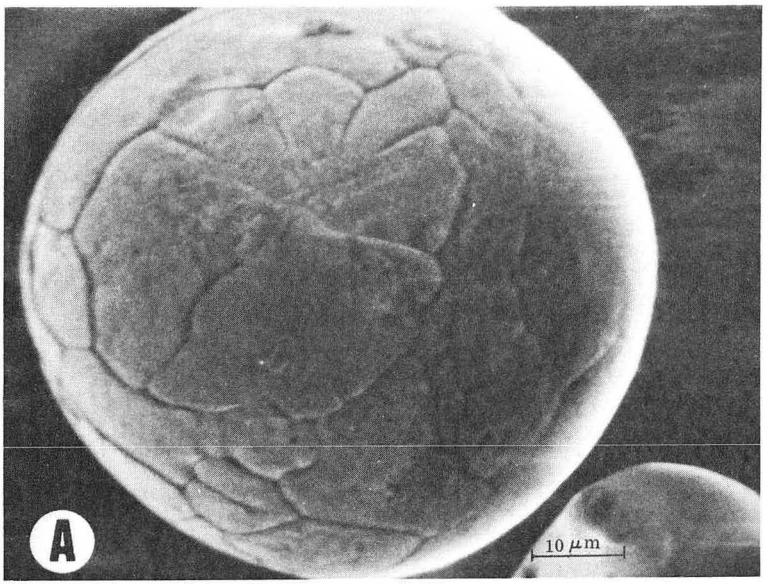


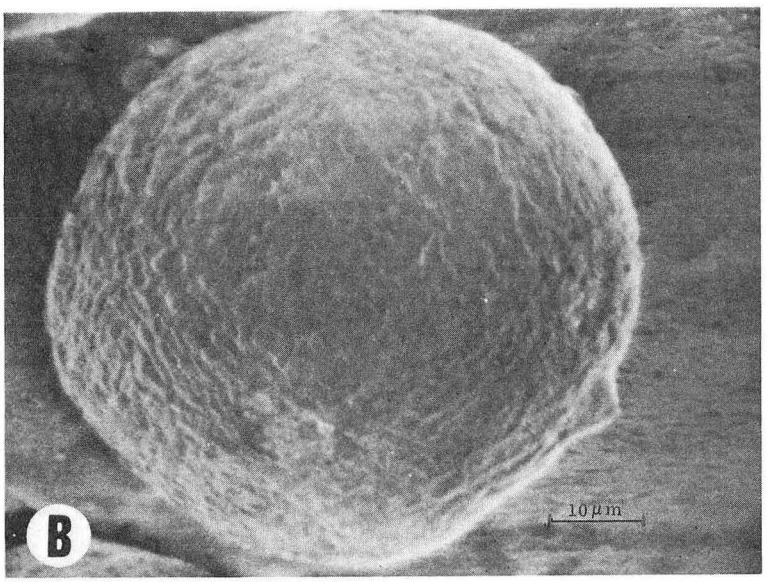


XBB 693-1887

Fig. 4

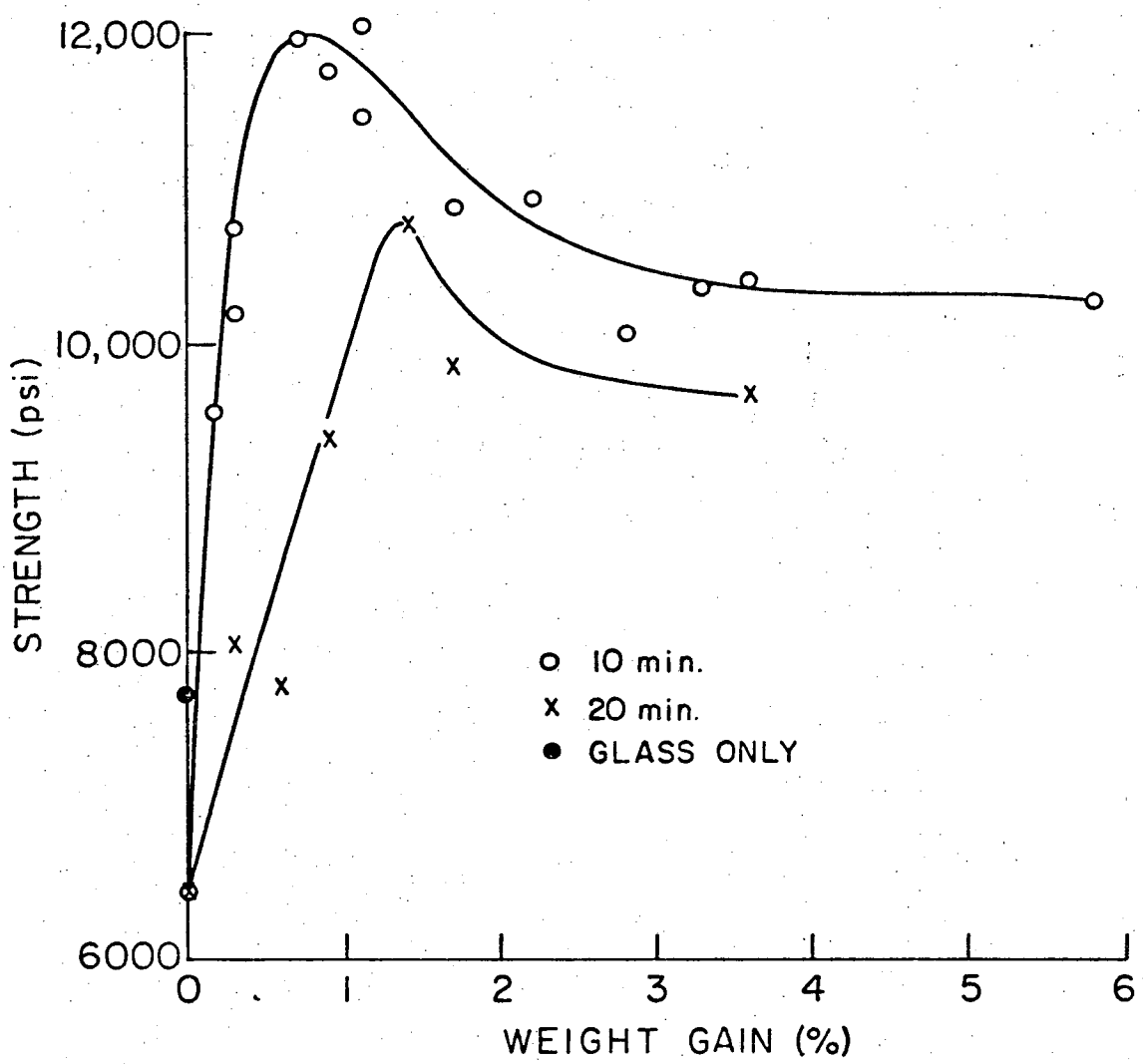


XBL 695-459

Fig. 5

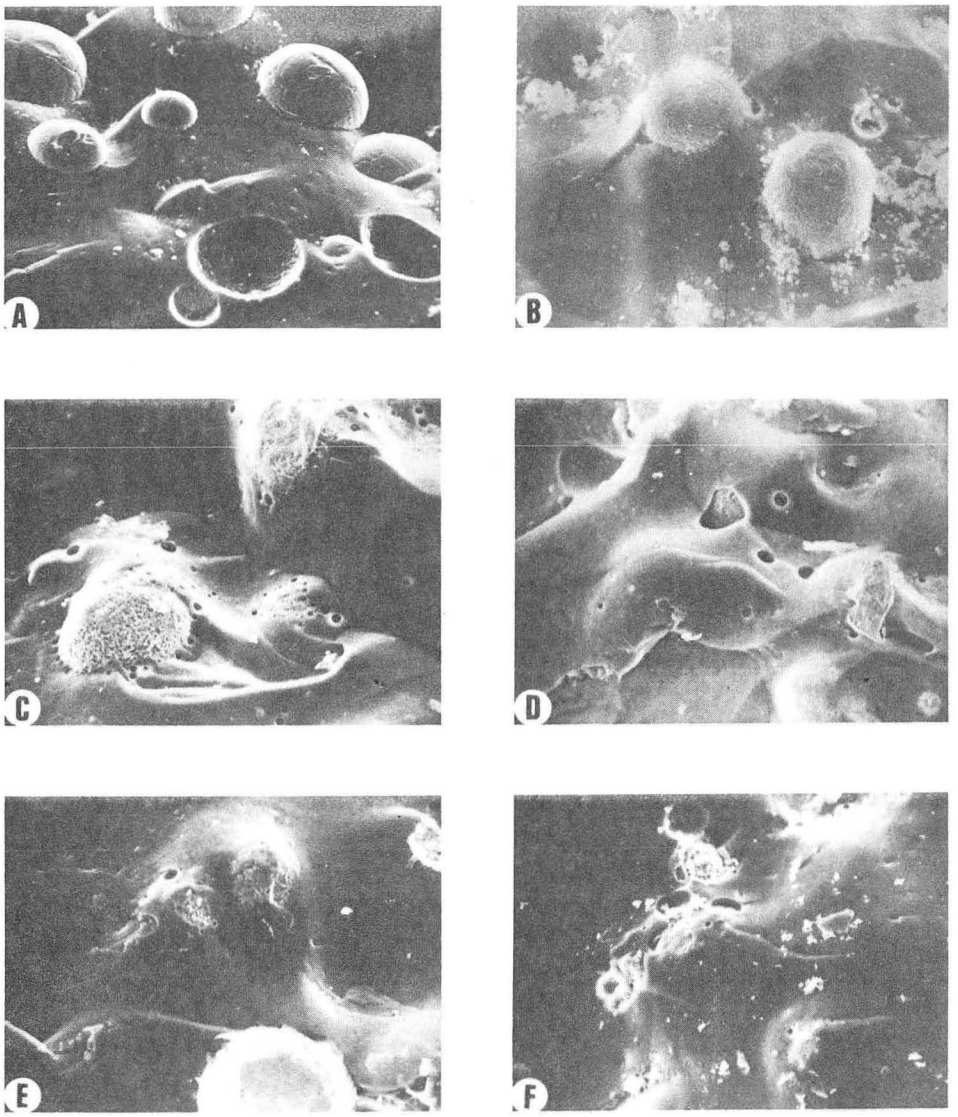


XBB 693-1889

Fig. 6

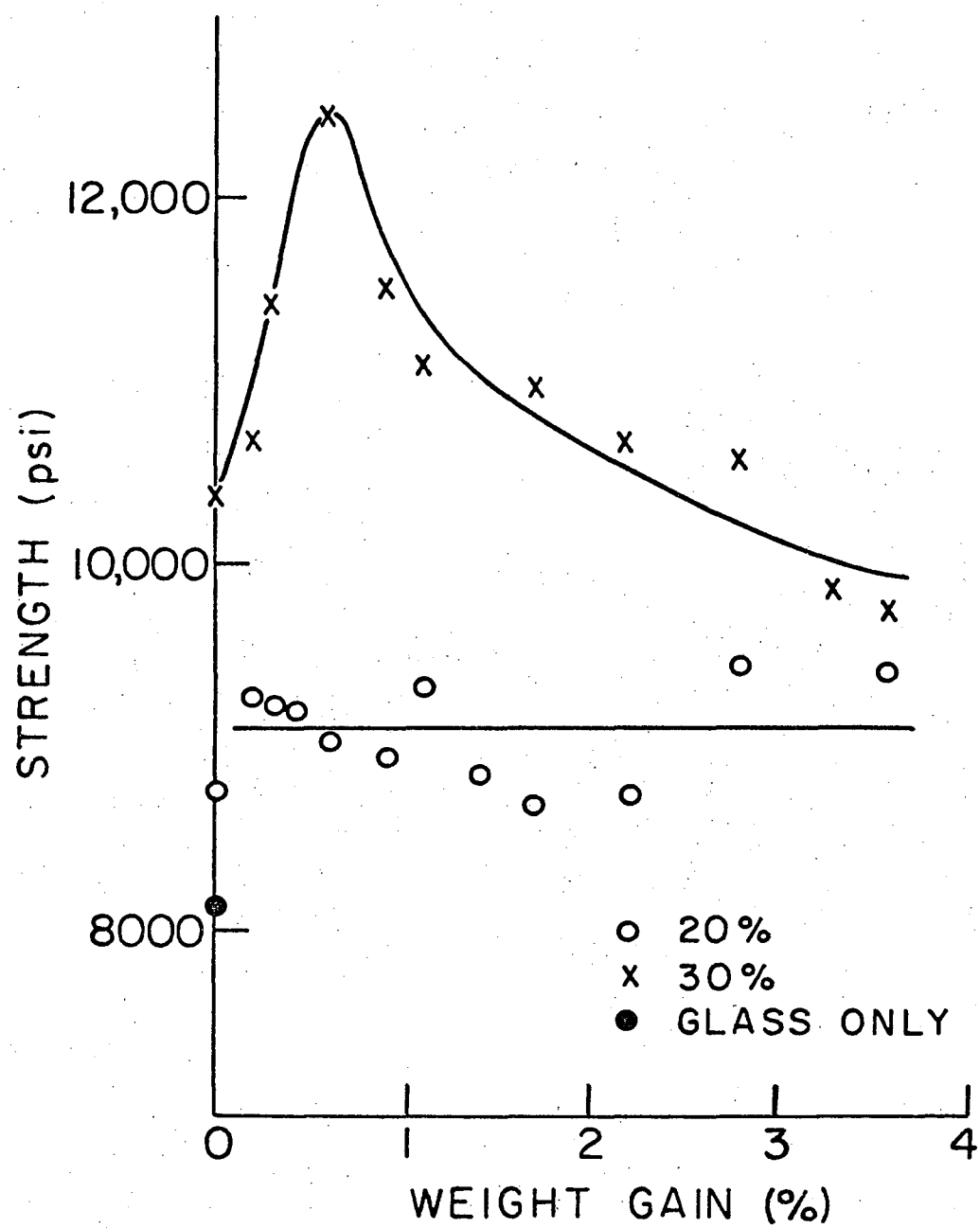


XBL 695-452

Fig. 7

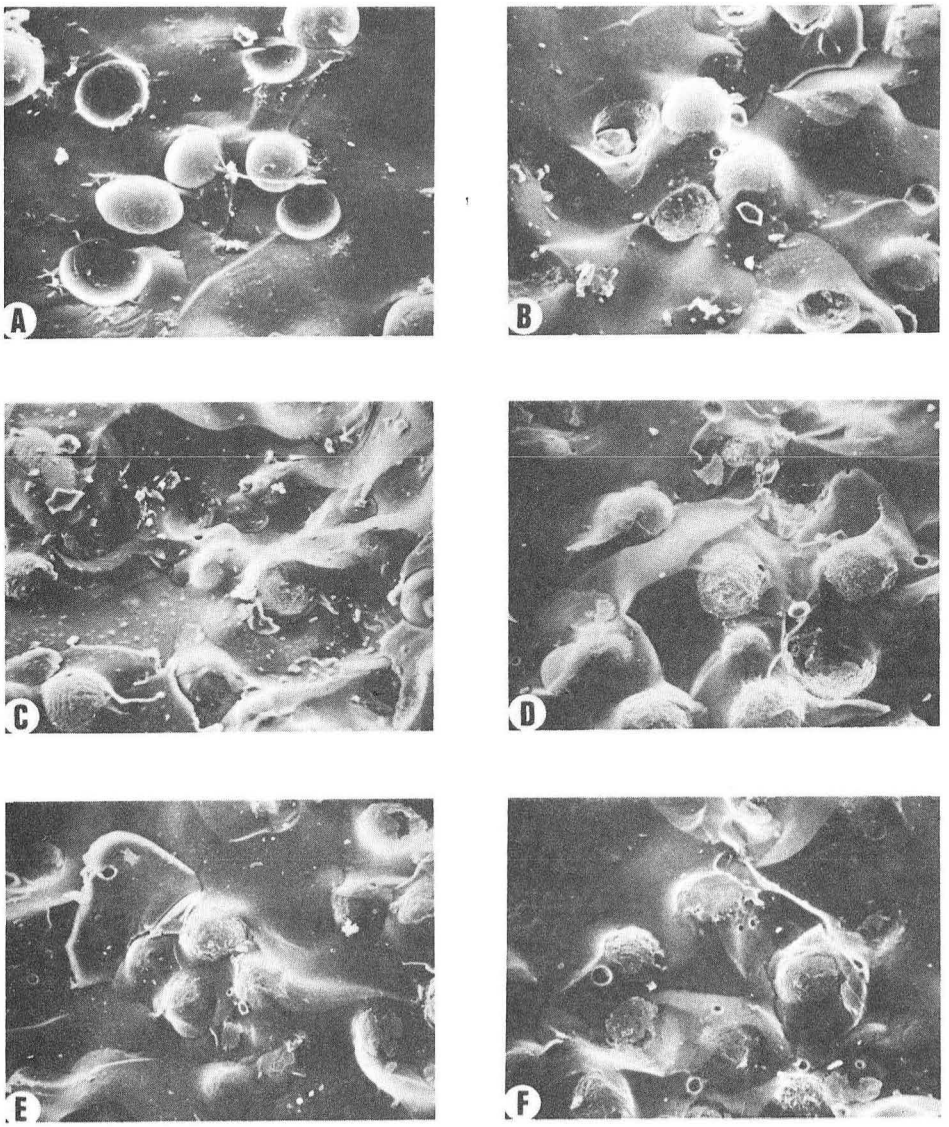


XBB 693-1886

Fig. 8

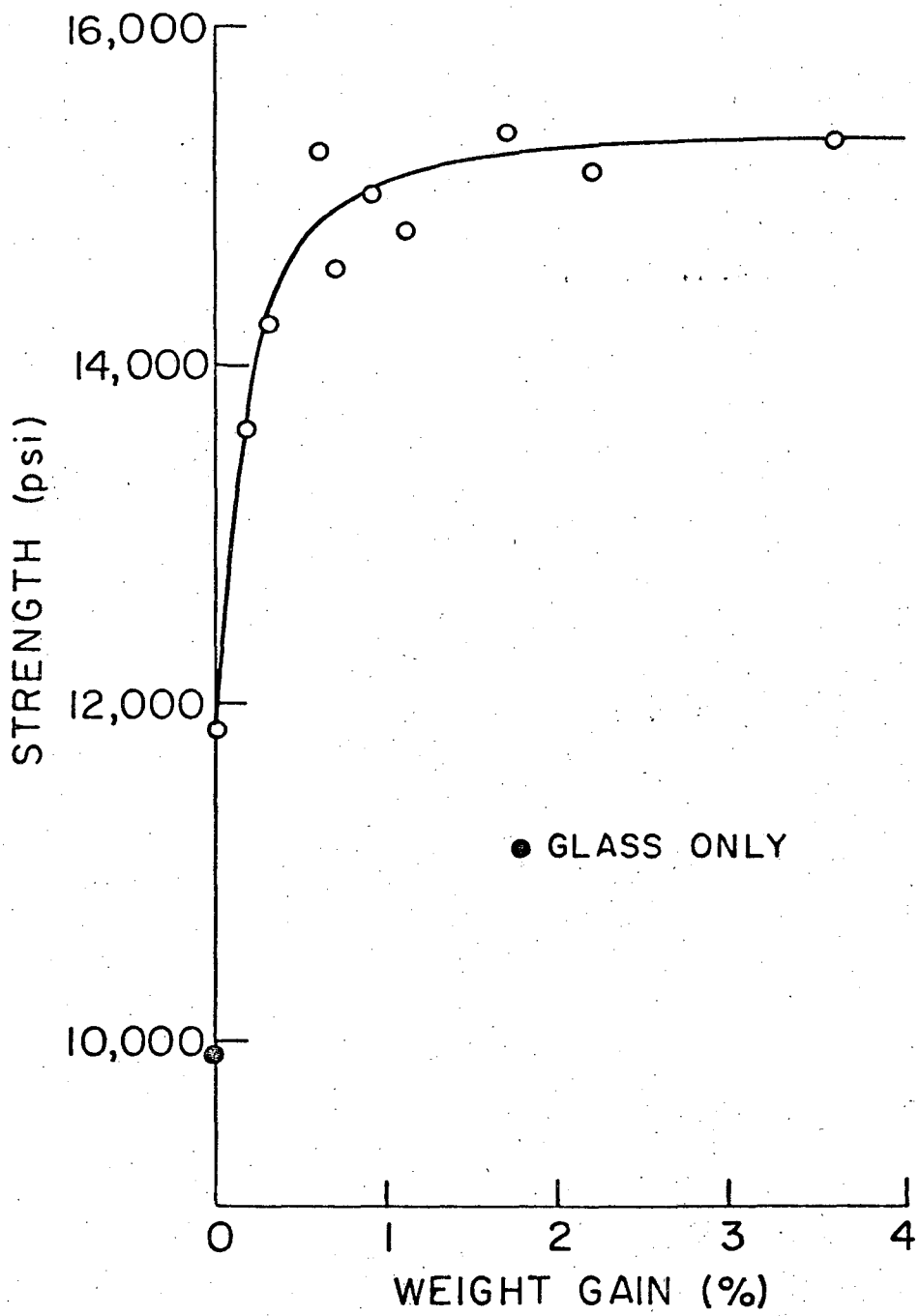


XBL 695-453

Fig. 9

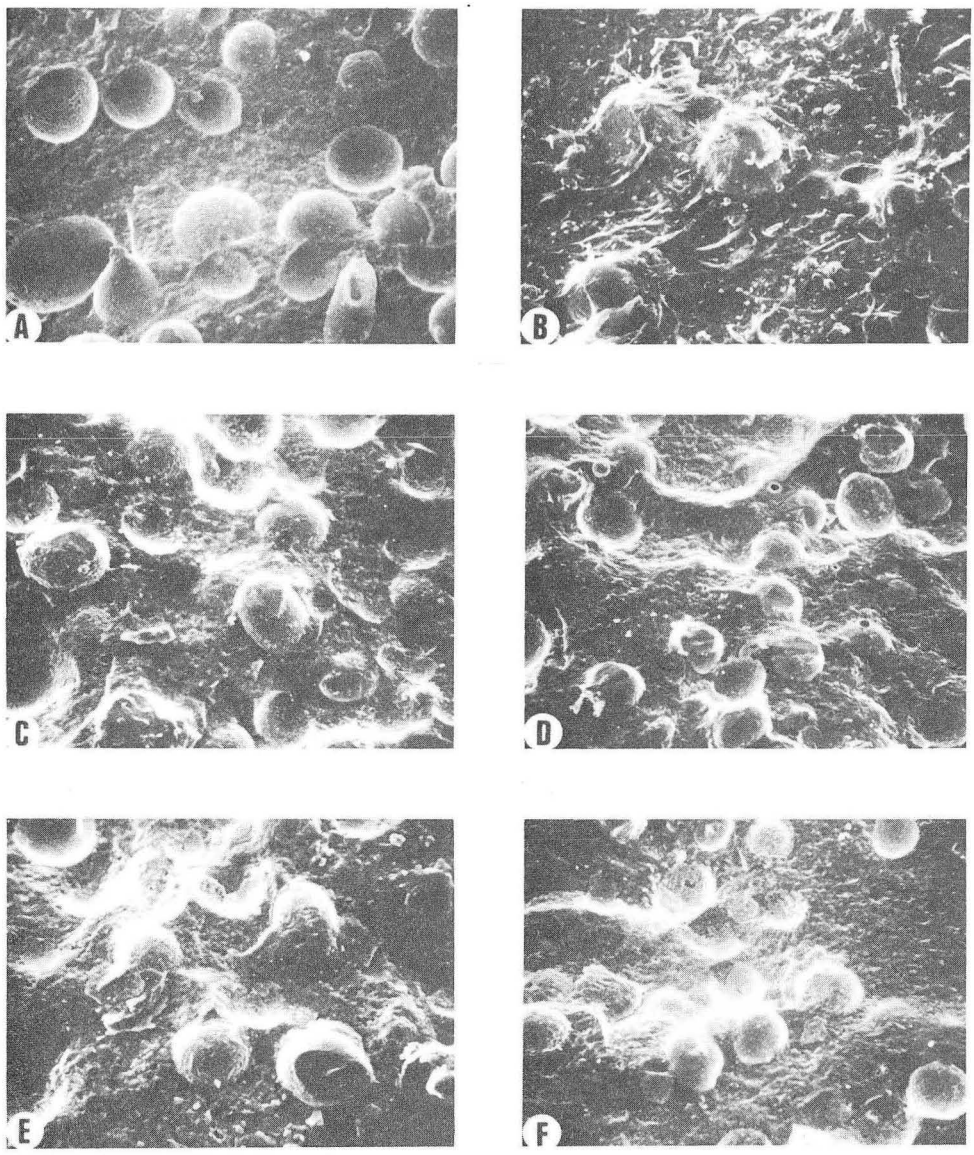


XBB 693-1888

Fig. 10

LEGAL NOTICE

*This report was prepared as an account of Government sponsored work. Neither the United States, nor the Commission, nor any person acting on behalf of the Commission:*

*A. Makes any warranty or representation, expressed or implied, with respect to the accuracy, completeness, or usefulness of the information contained in this report, or that the use of any information, apparatus, method, or process disclosed in this report may not infringe privately owned rights; or*

*B. Assumes any liabilities with respect to the use of, or for damages resulting from the use of any information, apparatus, method, or process disclosed in this report.*

*As used in the above, "person acting on behalf of the Commission" includes any employee or contractor of the Commission, or employee of such contractor, to the extent that such employee or contractor of the Commission, or employee of such contractor prepares, disseminates, or provides access to, any information pursuant to his employment or contract with the Commission, or his employment with such contractor.*

*TECHNICAL INFORMATION DIVISION*
*LAWRENCE RADIATION LABORATORY*
*UNIVERSITY OF CALIFORNIA*
*BERKELEY, CALIFORNIA 94720*